

# FIXED TUNES FAST CYCLING PERMANENT MAGNET PROTON FFA SYNCHROTRON\*

S. Brooks<sup>†</sup>, D. Trbojevic, F. Meot, and J. S. Berg, Brookhaven National Laboratory, Upton, USA

## Abstract

We present a novel concept of the Fixed-Field-Alternating (FFA) permanent magnet small racetrack proton accelerator with kinetic energy range between 10-250 MeV of. The horizontal and vertical tunes are fixed within the energy range providing very fast cycling with a frequency of 400Hz to 1.3 KHz. The injector is commercially available cyclotron with RF frequency of 65 MHz. The permanent magnet synchrotron has a shape of a racetrack where the two arcs are made of combined function permanent non-linear fields magnets to provide fixed betatron tunes for the extraordinary kinetic energy range between 10 and 250 MeV.

## INTRODUCTION

Sustainability is recently getting significant attention. US Department of Energy supports studies on energy efficient devices including particle accelerators. We are updating the previous report [1] on a new way to accelerate particles in the Fixed Field Alternating Gradient (FFA's) accelerator. This is a direct connection to sustainability and energy conservation as using the permanent magnets there is no need for electrical power. The synchrotron is based on an existing patent of the non-scaling FFA's (NS-FFA's) accelerator [2]. The linear transverse magnetic field of NS-FFA's is replaced with the non-linear field. This concept is based on a recent very successful commissioning [3-8] of the first 4 turn superconducting Energy Recovery Linac (ERL) 'CBETA' a collaboration between Cornell University and Brookhaven National Laboratory (BNL) in building Electron Test Accelerator. The CBETA project was funded by the New York State Energy & Research Development Authority (NYSERDA). A single NS-FFA's beam line very successfully transported 7 electron passes 4 accelerating and 3 decelerating passes with 42, 78, 114, and 150 MeV. The beam line was made of a very high-quality combined function magnets based on the Halbach design. A new permanent magnet technology was developed [5] allowing the initial beam to pass through without corrections. A concept of NS-FFA's [9-11] has been successfully demonstrated by other examples like: Electron Model for Multiple Applications (EMMA) at Daresbury Laboratory, UK [12] and by the experiment of a single NS-FFA's beam line transporting electrons with energies between 20-80 MeV at Advance Test Facility (ATF) at BNL [13]. The NS-FFA's abandoned the scaling laws like  $p = p_0(r/r_0)^{k-1}$  and  $B_R = B_0(r/r_0)^k$  where  $p$  is the momentum

of the accelerated particles while  $r$  is the radial particle offset. The  $B_R$  is the radial magnetic field dependence on radial offsets. They define the scaling FFA. The main advantage of the NS-FFA's with respect to the scaling FFA's are significantly smaller magnets. This is due to smaller orbit oscillations during acceleration a consequence of the very strong focusing reducing values of the dispersion function. From a definition of the dispersion function and a relationship between the orbit offsets and momentum range  $\Delta x = D_x \delta p/p$  it becomes clear that for the momentum range, for example of  $\delta p/p = \pm 60\%$  that orbit offsets could be within few cm for a dispersion function of less than  $D_x < 2\text{cm}$ . The scaling FFA's require 1/3 of the bending to be in opposite direction reducing the accelerator packing factor. This is another advantage of the NS-FFA's. Acceleration in the NS-FFA's needs to be fast or with a small number of passes as it was shown in the previous examples. As the NS-FFA accelerator is made of multiple identical cells there is a problem of crossing systematic resonances where the beam loss can occur. The beam loss depends on the length of time for the resonance crossing [13]. To avoid the resonance crossing we introduced the non-linear transverse magnetic field with a goal of obtaining the fixed betatron tunes and enhanced advantages of the strong focusing NS-FFA's.

## MAGNETIC FIELD EXPANSION

Additional multipoles are added to the combined function magnets using first the Taylor expansion of the magnetic field. The region of interest does not include electric currents so using the scalar potential  $\phi_m$  is best for treatment. The Laplace equation is satisfied [14, 15]:

$$\vec{\nabla}^2 \phi_m = 0 \quad \text{and} \quad \vec{B} = -\mu_0 \vec{\nabla} \phi_m \quad (1)$$

$$\phi_m = \phi_0 + \sum_{k=1}^{\infty} r^k (a_k \cos k\theta + b_k \sin k\theta) \quad (2)$$

$$-\frac{\Delta B_y}{B\rho} = -\frac{\partial \phi_m}{\partial x}, \quad \frac{B_x}{B\rho} = -\frac{\partial \phi_m}{\partial y} \quad (3)$$

The Hamiltonian has additional term [16]:

$$\Delta\phi \equiv \phi(x_T, y_T; s) - \phi(x_C, y_C; s) \quad (4)$$

where the potential difference is between the potential at the closed orbit at the reference energy  $E_C$  with the potential at the orbit at the energy  $E_T$ . The magnetic field projections on the rectangular place in x and y are:

$$B_y + iB_x = B_0 \sum_{k=1}^{\infty} (b_k + ia_k) \left( \frac{x+iy}{r_0} \right)^{k-1} \quad (5)$$

$$B_y = \sum_{k=0}^{\infty} \frac{b_k}{k!} x^k \quad \text{transverse vertical field} \quad (6)$$

\* This manuscript has been authored by employees of Brookhaven Science Associates, LLC under Contract No. DE-SC0012704 with the U.S. Department of Energy.

<sup>†</sup>sbrooks@bnl.gov

where the multipole coefficient we limited up to the 14<sup>th</sup> pole or  $k=7$ . The  $x$  is the distance on the transverse axis and  $B_0$  is the dipole magnetic field. The bending field values of the two combined function magnets, at the reference energy, were the same  $B_{0C}=0.54862\text{T}$  defining the reference radius of  $R_{0C}=3.5\text{ m}$ . In the example we present the reference proton kinetic energy is  $E_{kC}=129\text{ MeV}$ .

## TUNE DEPENDENCE ON MULTipoles

The effect of additional magnetic multipoles on the betatron tune variations has been widely investigated. We follow closely the previous works [15] where the tune variation dependence on the magnetic field  $\Delta\nu_x$  and  $\Delta\nu_y$  are functions of the offsets to the equilibrium orbit  $x_C$  at reference energy  $E_{kC}$  of a particle in the radial direction. If the vertical closed orbit could be ignored,  $y_C = 0$ , skew components  $a_k$ 's do not contribute to the tune shifts [16]. We varied the multipole components up to the 12<sup>th</sup> pole. The tune dependence on multipoles is shown as [16]:

$$\begin{aligned}\delta\nu_x &= \frac{B_0 l}{2\pi B\rho} \beta_x (b_1 G_1 + b_2 2x_C G_1 + b_3 (3x_C^2 G_1 + G_3) + \\ &b_4 (4x_C^3 G_1 + 4x_C G_3) + b_5 \cdot (5x_C^4 G_1 + 10x_C^2 + G_5)) \quad (7)\end{aligned}$$

$$\begin{aligned}\delta\nu_y &= \frac{B_0 l}{2\pi B\rho} \beta_x (b_1 H_1 + b_2 2x_C H_1 + b_3 (3x_C^2 H_1 + H_3) + \\ &b_4 (4x_C^3 H_1 + 4x_C H_3) + b_5 \cdot (5x_C^4 H_1 + 10x_C^2 + H_5)) \quad (8)\end{aligned}$$

where the coefficients  $G_i$  and  $H_i$  were previously defined [16] as:

$$G_1 = 1/2, G_3 = (3/8)\beta_x \varepsilon_x - (3/4)\beta_y \varepsilon_y,$$

$$G_5 = \frac{5}{16}(\beta_y \varepsilon_y)^2 + \frac{15}{8}(\beta_x \varepsilon_x \beta_y \varepsilon_y) + \frac{15}{16}(\beta_y \varepsilon_y)^2 \quad (9)$$

$$H_1 = -1/2, H_3 = -(3/4)\beta_x \varepsilon_x + (3/8)\beta_y \varepsilon_y,$$

$$H_5 = -\frac{5}{16}(\beta_y \varepsilon_y)^2 + \frac{15}{8}(\beta_x \varepsilon_x \beta_y \varepsilon_y) - \frac{15}{16}(\beta_y \varepsilon_y)^2 \quad (10)$$

A compilation of the non-linear magnetic field in NS-FFA's starts with a selection of the bending fields and gradients in the two combined function magnets such that a stable reference orbit is obtained for the selected horizontal and vertical tunes  $\nu_{xC}$  and  $\nu_{yC}$ . This defines the two magnetic multipoles coefficients  $b_{1x}$  and  $b_{1y}$ . To obtain equal maximum values of the magnetic field in focusing-**F** and defocusing-**D** magnet the *reference energy*  $E_C$  needs to be properly selected. Stable orbits must exist for each energy within the range. Many steps in energies above and below the reference energy  $E_{kC}$  are used to minimize a difference between the tunes, corresponding to other than reference energy  $E_{ki}$ :  $\Delta\nu_{xi} = (\nu_{xRi} - \nu_{xC}) \rightarrow 0$  and  $\Delta\nu_{yi} = (\nu_{yRi} - \nu_{yC}) \rightarrow 0$ . We adjusted the magnetic multipole coefficients above  $b_{1x}$  and  $b_{1y}$  up to the 14<sup>th</sup> pole or  $k=7$ . For each energy there must exist a stable orbit with radial offsets as previously labeled  $x_T$ . The stable orbits in a wide energy range are obtained by adjustments of the **F** and **D** sextupoles and additional multipoles. The reference energy orbit is circular within the two focusing and defocusing combined magnets while orbits of other energies oscillate

around the reference energy orbit. The maximum orbit offsets in the magnets are located at the minimum and maximum energies within the energy span. The proton kinetic energy range in this example was selected between 10 and 250 MeV.

## Transverse Magnetic Field Dependence: Taylor expansion replaced with the Fourier series

Fixed betatron tunes were obtained within the whole energy range by adjusting the magnetic multipoles defined by the Taylor expansion as shown by equations (5) and (6). Unfortunately, the results were showing small variations in tunes especially at lower energies. To avoid ill-conditioned optimization with high-order polynomials, the body field function is defined using a Fourier series [17]:

$$g(x) = c_0 + \sum_{n=1}^8 s_n \sin(nkx) + c_n \cos(nkx), \quad (11)$$

where  $k$  is a transverse scale factor and  $c_0 \dots c_8$  are the coefficients defining the field (units Tesla). The values of these coefficients [17] are provided in Table 1.

Table 1: Fourier Coefficients for the Magnet Body Fields

n	Magnet F, $k=60\text{ (m}^{-1}\text{)}$		Magnet D, $k=60\text{ (m}^{-1}\text{)}$	
	$c_n\text{ (T)}$	$s_n\text{ (T)}$	$c_n\text{ (T)}$	$s_n\text{ (T)}$
0	-0.69803	-	$c_n\text{ (T)}$	$s_n\text{ (T)}$
1	0.07561	1.73518	0.98934	-
2	0.30509	-0.44226	-1.91338	-2.46075
3	-0.13953	0.08267	0.39756	0.493241
4	0.02768	-0.02081	-0.13952	-0.13428
5	-0.00196	0.01916	0.01161	0.07066
6	0.00342	-0.01124	-0.01078	0.00724
7	-0.00265	0.002711	0.02076	-0.04809
8	0.00390	-6.57E-05	-0.01478	0.03069

## ORBIT DEPENDENCE ON ENERGY

The stable orbits within the two combined function magnets at kinetic energies between  $E_{kmin}=10\text{ MeV}$  and  $E_{kmax}=250\text{ MeV}$  are presented in Fig. 1.

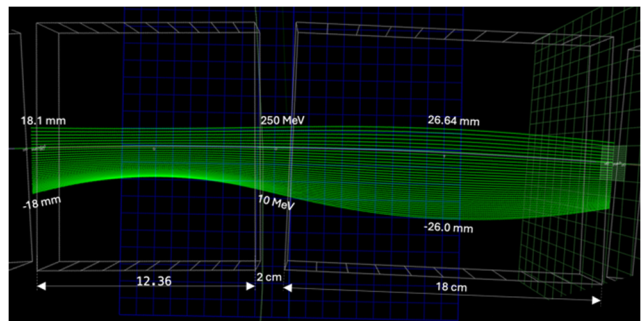


Figure 1: Proton beam orbits 10-250 MeV

A dependence shows that the orbit offsets are smaller in the defocusing magnet. A drift between the combined function magnets is selected to be 2 cm. Both magnets are rectangular sector magnets, and their maximum field is optimized to have the same values of  $|B_{max}|=1.86\text{ T}$ .

## Importance of the Fringe Field Dependence

A correct fringe fields are critical in the tune calculations as the magnet sizes and bending radii are very small. It was found that functions of the form [17]:

$$f(z) = \frac{\frac{1}{a} \arctan\left(\frac{z}{a}\right) - \frac{1}{b} \arctan\left(\frac{z}{b}\right)}{\left(\frac{1}{a} - \frac{1}{b}\right)\pi} + \frac{1}{2} \quad (12)$$

are very good fit to the real permanent magnet fringe fields measurements. Both magnets in this cell use values  $a = 0.02\text{ m}$  and  $b = 0.04\text{ m}$ . The effect of the fringe fields is shown in Fig. 2. Both the proton beam orbits, and magnetic fields of both magnets are shown.

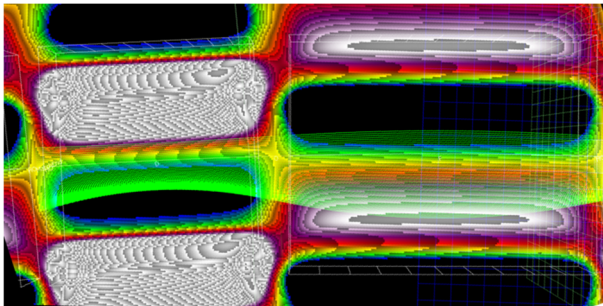


Figure 2: Orbit in D and F magnets with magnetic fields.

## Magnetic Transverse Field Dependence

The magnetic field at the cross section of both defocusing and focusing magnets is shown in Fig. 3. The synchrotron design starts with an accurate estimate of the beam size. The orbit variations within the non-linear magnetic field need to consider the beam size. This is especially important for the magnetic field variation of the focusing magnet at lower energy range. The dynamical aperture studied in the whole energy range shows a smaller value at lower energy range due to the largest value of the beam size. As the beam is accelerated the beam size is reduced due to momentum increase.

## Betatron Tune Dependence on Kinetic Energy

Results for the tune dependence on kinetic energy are shown in Fig. 3.

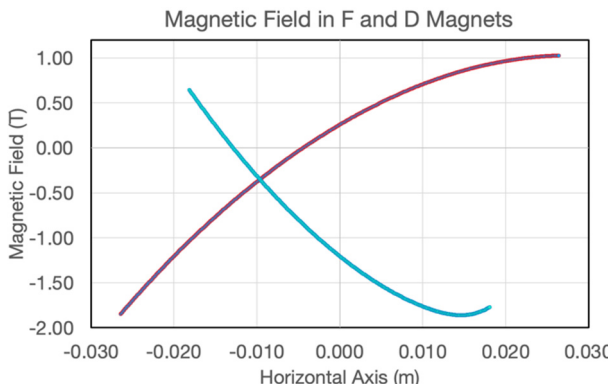


Figure 3: Magnetic field dependence on the transverse distance in F (red) and D (blue) magnets in the basic cell.

## Permanent Magnet Design

The permanent magnet design is based on already developed technology during the CBETA project. The BNL provided a funding through the Laboratory Directed Research & Development (LDRD) to build a part of the fast-cycling permanent magnet synchrotron. The cross section of the focusing **F** and defocusing **D** magnets are shown in Fig. 4.

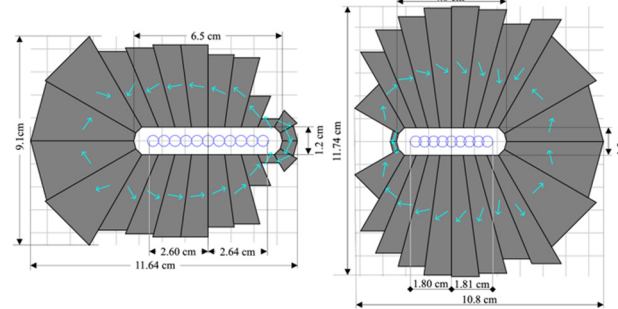


Figure 4: Cross sections of the permanent F (left) and D (right) non-linear magnets.

## Betatron Tune Dependence on Energy

The recent optimization results on tune dependence on energy, obtained using the Fourier series, are shown in Fig. 5.

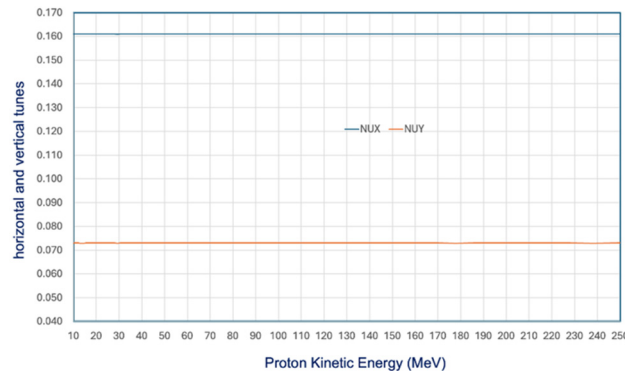


Figure 5: Betatron Tunes dependence on proton kinetic energy for the permanent magnet fast cycling synchrotron.

## SUMMARY

A non-linear FFA's permanent magnet fast cycling proton accelerator is presented. This work follows the successful commissioning of the CBETA project with a proof of using the linear FFA's. The results shown are significant for future particle accelerators, proton drivers and colliders from multiple points: saving in energy as the magnetic field is fixed in this case permanent magnets are used and there is no need for pulsing the magnets creating a possibility for fast cycling accelerators as the **RF** is the only remaining limitation. The proton drivers for the muon collider could be built by using the combined function superconducting magnets as already shown by L. Brouwer [18]. The presented proton accelerator is made for the cancer FLASH therapy as it is possible to deliver required radiation dose in a very short time is shown at this conference [19].

## REFERENCES

[1] D. Trbojevic, J. S. Berg, M. Blaskiewicz, and S. J. Brooks, “Fast Cycling FFA Permanent Magnet Synchrotron”, in *Proc. IPAC’22*, Bangkok, Thailand, Jun. 2022, pp. 126-129. doi:10.18429/JACoW-IPAC2022-MOPST02

[2] D. Trbojevic, “Non-Scaling Fixed Field Alternating Gradient Permanent Magnet Cancer Therapy Accelerator,” United States Patent Application Publication, Pub. No.: US 2014/0252994 A1, Sep. 11, 2014.

[3] A. Bartnik *et al.*, “CBETA: First Multipass Superconducting Linear Accelerator with Energy Recovery,” *Phys. Rev. Lett.*, vol. 125, no. 4, Jul. 2020. doi:10.1103/physrevlett.125.044803

[4] C. Gulliford *et al.*, “Measurement of the per cavity energy recovery efficiency in the single turn Cornell-Brookhaven ERL Test Accelerator configuration,” *Phys. Rev. Accel. Beams*, vol. 24, no. 1, Jan. 2021. doi:10.1103/physrevaccelbeams.24.010101

[5] S. Brooks, G. Mahler, J. Cintorino, J. Tuozzolo, and R. Michnoff, “Permanent magnets for the return loop of the Cornell-Brookhaven energy recovery linac test accelerator,” *Phys. Rev. Accel. Beams*, vol. 23, no. 11, Nov. 2020. doi:10.1103/physrevaccelbeams.23.112401

[6] D. Trbojevic, R. Michnoff and G. Hoffstaetter *et al.*, “CBETA Project Report,” CLASSE, Ithaca, New York, NYSERDA contract No. 102192, March 2020.

[7] D. Trbojevic, J. S. Berg, S. J. Brooks, W. Lou, F. M?ot, and N. Tsoupas, “Multi Pass Energy Recovery Linac Design With a Single Fixed Field Magnet Return Line”, in *Proc. ICAP’18*, Key West, Florida, USA, Oct. 2018, pp. 191-195. doi:10.18429/JACoW-ICAP2018-TUPAF09

[8] K. E. Deitrick, A. Hutton, A. C. Bartnik, C. M. Gulliford, and S. A. Overstreet, “Novel Straight Merger for Energy Recovery Linacs”, in *Proc. LINAC’18*, Beijing, China, Sep. 2018, pp. 702-705. doi:10.18429/JACoW-LINAC2018-THP0010

[9] D. Trbojevic, E. D. Courant, and A. A. Garren, “Colliders and collider physics at the highest energies: Muon colliders at 10 TeV to 100 TeV: HEMC ’99 Workshop,” Bruce J. King, Ed. Montauk, New York: *AIP Conference Proceedings* 530, 27 September-1 October 1999.

[10] C. Johnstone, W. Wan, and A. Garren, “Fixed Field Circular Accelerator Designs”, in *Proc. PAC’99*, New York, NY, USA, Mar. 1999, paper THP50, pp. 3068-3070.

[11] D. Trbojevic, E. D. Courant, and M. Blaskiewicz, “Design of a nonscaling fixed field alternating gradient accelerator,” *Phys. Rev. Spec. Top. Accel Beams*, vol. 8, no. 5, May 2005. doi:10.1103/physrevstab.8.050101

[12] S. Machida *et al.*, “Acceleration in the linear non-scaling fixed-field alternating-gradient accelerator EMMA,” *Nat. Phys.*, vol. 8, no. 3, pp. 243–247, Jan. 2012. doi:10.1038/nphys2179

[13] K. M. Walsh, “Fixed-field accelerator transports multiple particle beams at a wide range of energies through a single beam pipe”, <https://phys.org/news/2017-08-fixed-field-multiple-particle-wide-range.html>

[14] D. Trbojevic, M. Blaskiewicz, and E. Forest, “Crossing Resonances in a Non-Scaling FFAG,” *Int. J. Mod. Phys. A*, vol. 26, no. 10n11, pp. 1852–1864, Apr. 2011. doi:10.1142/s0217751x11053249

[15] D. Trbojevic, “Magnetic Measurements of the Correction and Adjustment Magnets of the Main Ring”, Fermilab TM-1412, 1986, <https://inspire-hep.net/files/2a08535a36b3c639c55d67a25d5bb14d>

[16] S. Ohnuma, “Shifts in Betatron Oscillation Frequencies Carried by Average Multipole Fields”, Fermilab, FERMILAB-PBAR-NOTE-324, Jul. 1983.

[17] Stephen Brooks, Dejan Trbojevic, “Benchmark Midplane Field for Medical FFA”, Brooks Reports, April 2, 2024, <https://stephenbrooks.org/ap/report/2024-5/benchmark.pdf>

[18] L. Brouwer, “Producing circular field harmonics inside elliptic magnet apertures with superconducting canted-cosine-theta coils,” *Phys. Rev. Accel. Beams*, vol. 27, no. 2, Feb. 2024. doi:10.1103/physrevaccelbeams.27.022402

[19] D. Trbojevic and S. Brooks, “FLASH proton therapy facility design with permanent magnets”, presented at the IPAC’24, Nashville, TN, USA, May 2024, paper THPR46, this conference.